

Disclaimer/Publisher's Note: The statements, opinions, and data contained in all publications are solely those of the individual author(s) and contributor(s) and not of MDPI and/or the editor(s). MDPI and/or the editor(s) disclaim responsibility for any injury to people or property resulting from any ideas, methods, instructions, or products referred to in the content.

Asymmetries in strong solar flares

Eugene Bagashov^{1*}

¹Independent Researcher, 97–28 Lobanka str., Minsk 220019, Belarus

Accepted XXX. Received YYY; in original form ZZZ

ABSTRACT

The details of the solar flare production mechanisms are not yet completely understood. One of the standing questions is the anisotropy of the X-ray flux, especially in strong flares. It can be studied indirectly by analysing the characteristics of flares at different positions on the visible disc. In this paper, the durations, peak and integral fluxes of strong (X-class) solar flares from cycles 22–25 are considered with respect to their apparent position on the Sun. It is found that there exists a significant north–south asymmetry in all three parameters, which also varies depending on the phase of the solar cycle (with general predominance of the south). This confirms the results of previous studies. A weaker and less significant east–west asymmetry is found as well, partly supported by literature. A previously undetected centre-to-limb asymmetry is reported (in favour of the limb) in all three parameters. All three asymmetries are enhanced during the solar minimum, which could hint at their connection to the large scale magnetic structuring of the Sun. The prevalence of strong solar flares near the limb at the solar minimum has clear space weather warning implications.

Key words: Sun: activity – Sun: flares – Sun: X-rays, gamma-rays

1 INTRODUCTION

In order to understand the mechanisms responsible for the production of strong solar flares, it is necessary to gather sufficient amounts of observational data. One particular property of interest is their possible directionality (anisotropy), which may be probed over the long periods of time even from a single point of observation (Earth and near-Earth space) by studying the flare properties versus their position on the visible solar disc.

The present work focuses on statistical evaluation of the possible asymmetries in strong solar flares in terms of their position: disc versus limb, north versus south, east versus west. Three parameters are being considered for comparison: solar flare duration, peak X-ray flux in 1–8 Å range, integral flux in the same range over the flare's duration.

2 METHODS

2.1 Reference flare list

The catalogue provided by [Plutino et al. \(2023\)](#) was used as a reference. Regarding the strong flares, the catalogue demonstrates some noteworthy properties:

- A few of the X-flares listed are clearly parts of the same event (apparently with more than one peak, separated by less than 30 minute time intervals). In these cases only the

strongest flare of the consecutive series was taken into account.

- The catalogue tends to overestimate the peak flux of each individual flare by 20–60% compared to the initial *GOES* satellite data (therefore being more in line with the modern nomenclature ([Machol et al. 2023](#)), where the historical 42% attenuation factor is removed). As it occurs consistently throughout the catalogue, no corrections to account for this have been made.

- For the same reason some of the X-flares listed in the catalogue correspond to “weaker” (M-class) *GOES* flares. Since the boundary between M and X classes is somewhat arbitrary, this is rather beneficial, as it increases the sample size.

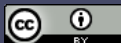
After 2020 the standard *GOES* catalogue was used ([NOAA 2023](#)).

2.2 Visual identification

The position of the solar flare on the visible disc was evaluated using the X-ray/EUV images of the flares (taken by *Yohkoh* ([Montana State University 2017](#)), *SOHO* ([Virtual Solar Observatory 2023](#)) and *SDO* ([Pesnell 2023](#)) satellites). Where such images were unavailable, the active region position was used as a proxy (using the synoptic maps from [NGDC \(2023\)](#) as a reference).

This is a necessary measure, as e.g. H α emissions are biased against the limb and therefore tend to underestimate the number of limb flares ([Conway & Matthews 2003](#)). The scope of the strong solar flares to be included is therefore limited by the availability of digital images of the Sun in shorter wave-

* E-mail: paladin17@yandex.by



2 *E. Bagashov*

lengths, which puts the start of the considered time interval at September of 1991.

To facilitate the identification of the flare position, the apparent grid of meridians and parallels was plotted and overlaid on top of the satellite imagery. The grid step is 9 degrees in both latitudinal and longitudinal directions. Longitudinal bins are numbered from -10 (easternmost) to $+10$ (westernmost). For latitudinal bins -10 represents the southern polar region, and $+10$ – the northern one.

Flares often happen near the bin boundaries, which makes the attribution of a flare to a certain bin number (versus the very next one) somewhat arbitrary. However, increase in resolution leads to a frequent “overflowing” (i.e. when a flare happens in more than one bin simultaneously), especially near the limb. Hence the choice has been made to limit the resolution to a 20 by 20 bin grid.

2.3 Processing of the list

As a result of the described procedure, the list of X-flares has been obtained. It includes data on: 1) date of the event; 2) time of the flare peak (UTC); 3) corresponding active region number; 4) peak flux of the flare; 5) longitude bin; 6) latitude bin; 7) a special note if the flare happened in the occulted active region (behind the limb); 8) flare duration; 9) integral flux of the flare over its duration.

Occultation is given special attention. As the flares often happen in coronal loops (Reale 2014), which are situated above the photosphere, they can sometimes still be visible after the active region has departed the Earth-facing disc (or before the active region has appeared on it), which effectively oversaturates the ± 10 longitude bins with extra flares, which introduces a bias in judgement about the uniformity of disc-limb flare number distribution. See discussion of the same issues by Krucker et al. (2015).

Finally, 3 lists have been produced: 1) the full list that contains all the X-flares (as described in section 2.1) from September 1991 to May 2023 – it includes 305 events; 2) the B-list where some of the flares from occulted active regions have been eliminated (the ones that definitely belong to the backside of the Sun) – it includes 288 events; 3) the maximally conservative M-list where even the flares at the very edge of the disc (that could be equally attributed to visible and occulted areas) have been eliminated – it includes 274 events.

2.4 Temporal breakdown

In order to determine the possible temporal differences, a set of smaller lists was produced: the solar minimum list, the solar maximum list, the rising and falling phase lists, odd and even cycle lists, and separate lists for flares from each solar cycle at least partly included in the study (cycles 22–25).

For the purposes of this research, a solar maximum (minimum) is defined as a year with maximum (minimum) sunspot count of the corresponding cycle, plus 2 full years before and after it. Hence the solar maximum (minimum) list includes the strong flares from years 1991, 1999–2003, 2012–2016, 2022–2023 (1994–1998, 2006–2010, 2017–2021). For the purposes of this research, the rising phase is defined as all the full years between the years with minimum and maximum sunspot count (i.e. the years 1997–2000, 2009–2013, 2020–2023). For the purposes of this research, the falling phase is

Table 1. Cumulative characteristics of the acquired lists: the name of the list, total number of flares N in it, mean duration of the flares T , mean peak flux F , mean integral flux I . N values are taken from the full list (values in parentheses – from the M list).

List	N	T (min)	F (10^{-4} W·m $^{-2}$)	I (J·m $^{-2}$)
Full	305	129.7	2.92	0.502
B	288	125.7	2.89	0.478
M	274	125.2	2.84	0.463
Min	37 (32)	122.0	3.47	0.409
Max	193 (175)	122.7	2.88	0.472
Rise	104 (91)	114.5	2.36	0.318
Fall	141 (126)	128.3	3.08	0.535
Odd	195 (177)	120.6	3.12	0.498
Even	110 (97)	133.6	2.31	0.398
C22	36 (31)	117.3	2.33	0.399
C23	179 (163)	125.7	3.27	0.532
C24	74 (66)	141.2	2.31	0.397
C25	16 (14)	61	1.44	0.105

defined as all the full years between the years with maximum and minimum sunspot count (i.e. the years 1991–1995, 2002–2007, 2015–2018).

It is worthy to note that the years 1994, 2008–2010, 2018–2020, even though they are technically included into consideration everywhere where they should, have had no strong solar flares.

Summary of the acquired lists is given in Table 1. The flare numbers in parentheses indicate the ones taken from the M-list (to evaluate the disc-limb flare number difference).

3 ACQUIRING THE STATISTICS

3.1 Asymmetry indices

For a quick and uniform description of the observed centre-to-limb, north-south and east-west differences, asymmetry indices are introduced (analogous to the ones in e.g. Roy (1977)):

$$\alpha_x = \frac{x_1 - x_2}{x_1 + x_2}, \quad (1)$$

where x is one of the considered values (number of flares N , mean flare duration T , mean peak flux F , mean integral flux I) and the different subscripts correspond to different areas under consideration depending on the context (“1” denotes limb/north/west, and “2” – disc/south/east). E.g. $\alpha_F = (F_1 - F_2)/(F_1 + F_2)$ may denote the asymmetry index describing the north-south differences in mean peak flare flux.

As follows from (1), the ratio x_1/x_2 (e.g. mean north peak flux divided by mean south peak flux) and the fraction of the total $\beta = x_1/(x_1 + x_2)$ can be acquired from the appropriate α_x value in the following way:

$$\frac{x_1}{x_2} = \frac{1 + \alpha_x}{1 - \alpha_x}, \quad \beta = \frac{1 + \alpha_x}{2}. \quad (2)$$

Table 2 shows the centre-to-limb asymmetry indices (positive values in favour of the limb) calculated for all the considered lists. As discussed in section 2.3, the number asymmetry for the temporal breakdown lists is taken with respect to the maximally conservative M list. In Table 3 the north-south

Table 2. Centre-to-limb asymmetry indices regarding the flare number α_N , mean flare duration α_T , mean peak flux α_F , and mean integral flux α_I (positive in favour of the limb).

List	α_N	α_T	α_F	α_I
Full	0.102	0.053	0.099	0.123
B	0.048	0.027	0.095	0.085
M	0.0	0.024	0.083	0.059
Min	0.312	-0.139	0.137	0.074
Max	-0.018	-0.001	0.020	-0.042
Rise	0.142	0.026	0.036	-0.038
Fall	0.0	0.111	0.087	0.148
Odd	-0.028	0.037	0.143	0.135
Even	0.052	-0.003	-0.046	-0.104
C22	0.096	-0.058	-0.104	-0.055
C23	-0.068	0.058	0.166	0.165
C24	0.030	0.022	-0.020	-0.128
C25	0.428	0.044	0.111	0.296

Table 3. North-south asymmetry indices regarding the flare number α_N , mean flare duration α_T , mean peak flux α_F , and mean integral flux α_I (positive in favour of the north).

List	α_N	α_T	α_F	α_I
Full	-0.128	-0.031	-0.102	-0.148
B	-0.132	-0.006	-0.087	-0.105
M	-0.132	0.010	-0.070	-0.067
Min	-0.298	-0.070	-0.250	-0.316
Max	-0.160	-0.096	-0.042	-0.140
Rise	0.250	0.012	0.049	0.192
Fall	-0.290	-0.016	-0.214	-0.221
Odd	-0.108	-0.062	-0.147	-0.193
Even	-0.164	0.024	-0.006	-0.061
C22	-0.278	0.042	0.047	0.031
C23	-0.118	-0.045	-0.148	-0.194
C24	-0.108	0.009	-0.029	-0.102
C25	0.0	-0.316	0.00	0.345

indices are given (positive values in favour of the north). And Table 4 outlines the east-west asymmetry indices (positive in favour of the west).

3.2 Flare statistics

In order to evaluate the statistical significance of the number asymmetry (given by the first column in Tables 2-4) a null-hypothesis is made that the distribution of flares should be uniform. A standard binomial test is performed to estimate the probability of the null-hypothesis to be true. The results are shown in Table 5. Notable values ($p < 0.15$) are highlighted in bold. Detailed analysis of the results is given in section 4.

In order to quantify the differences between the alternative samples (north/south etc.) of strong flares with respect to their durations, peak and integral fluxes, two-sample Kolmogorov-Smirnov test has been used. The only notable results that have been found (with significance level $\alpha < 0.2$) are summarized in the Table 6, sorted in descending order by α .

Another way of looking at the problem is estimating the correlation coefficients between longitude and latitude and

Table 4. East-west asymmetry indices regarding the flare number α_N , mean flare duration α_T , mean peak flux α_F , and mean integral flux α_I (positive in favour of the west).

List	α_N	α_T	α_F	α_I
Full	0.022	0.009	0.039	0.041
B	0.028	-0.004	0.025	0.004
M	0.008	0.001	0.073	0.058
Min	0.136	0.126	0.033	0.123
Max	0.046	-0.027	0.024	0.017
Rise	0.038	0.011	0.062	-0.025
Fall	-0.008	0.051	0.013	0.090
Odd	0.046	0.026	0.019	-0.027
Even	-0.018	-0.010	0.070	0.174
C22	-0.112	0.155	0.161	0.396
C23	0.040	0.035	0.023	-0.018
C24	0.028	-0.086	0.026	0.051
C25	0.126	-0.091	0.018	-0.295

Table 5. Binomial test p -values for the flare number asymmetries α_N in Tables 2-4.

List	p (disc-limb)	p (north-south)	p (east-west)
Full	0.043	0.015	0.366
B	0.222	0.015	0.340
M	0.524	0.017	0.476
Min	0.055	0.049	0.256
Max	0.440	0.015	0.282
Rise	0.104	0.007	0.384
Fall	0.535	0.0003	0.500
Odd	0.382	0.076	0.283
Even	0.342	0.052	0.462
C22	0.360	0.066	0.309
C23	0.217	0.067	0.327
C24	0.451	0.208	0.454
C25	0.090	0.598	0.402

Table 6. Results of Kolmogorov-Smirnov test for alternative sample differences in terms of flare durations T , peak fluxes F and integral fluxes I . In descending order of the last column.

N ^o	List	Samples	x	Significance level α
1.	Fall	East/west	T	< 0.2
2.	Odd	North/south	T	< 0.2
3.	Max	North/south	T	< 0.15
4.	Odd	North/south	I	< 0.15
5.	C23	North/south	I	< 0.15
6.	C24	East/west	T	< 0.1
7.	Max	Disc/limb	I	< 0.05
8.	Rise	North/south	I	< 0.05

the three values under consideration. For each of the lists given in Table 1 Pearson correlation coefficient r , Spearman's rank correlation coefficient ρ and Kendall's rank correlation coefficient τ have been calculated both for longitude and latitude (both in signed and absolute values). Kendall's τ have been found to be very close to Spearman's ρ (this is also true for their corresponding p -values) in every notable case, hence only the ρ value is given. On the other hand, Pearson's r is rarely similar (as well as the corresponding p), the main

Table 7. Pearson's r (with the corresponding p -value p_r) and Spearman's ρ (with p_ρ) coefficients for correlation between longitude (latitude) in absolute values and the flare duration T , peak flux F and integral flux I . In descending order of the last column.

N ^o	List	Lon/lat	x	r	p_r	ρ	p_ρ
1.	Fall	Lon	I	0.193	0.022	0.127	0.134
2.	Even	Lat	T	0.076	0.427	0.147	0.127
3.	Fall	Lat	T	-0.104	0.219	-0.129	0.126
4.	Full	Lat	T	-0.096	0.095	-0.098	0.087
5.	M	Lat	T	-0.105	0.083	-0.108	0.074
6.	Fall	Lon	F	0.141	0.095	0.153	0.071
7.	Fall	Lon	T	0.141	0.095	0.160	0.059
8.	C24	Lat	I	0.017	0.888	0.228	0.050
9.	Even	Lat	I	0.091	0.345	0.192	0.045
10.	B	Lat	T	-0.118	0.046	-0.122	0.039
11.	Min	Lon	F	0.265	0.112	0.345	0.037
12.	C23	Lat	T	-0.185	0.013	-0.186	0.012
13.	Odd	Lat	T	-0.184	0.010	-0.198	0.006

Table 8. Same as Table 7, but values of longitude and latitude are signed.

N ^o	List	Lon/lat	x	r	p	ρ	p_ρ
1.	Even	Lon	F	0.069	0.475	-0.139	0.145
2.	Max	Lat	T	-0.113	0.117	-0.105	0.144
3.	Max	Lon	F	0.054	0.455	-0.113	0.118
4.	Odd	Lat	T	-0.103	0.148	-0.117	0.105
5.	Min	Lon	T	-0.025	0.882	0.279	0.095
6.	C24	Lon	F	0.015	0.902	-0.217	0.063
7.	Rise	Lat	I	0.191	0.052	0.213	0.030

reasons for which are most likely that the samples are not normalized and contain significant outliers. It is given here for illustrative purposes. Tables 7 and 8 summarize the results (only the cases with $p_\rho < 0.15$ are shown).

4 RESULTS

4.1 Centre-to-limb asymmetry

Even though after the removal of the flares in the occulted regions (see section 2.3) the disc-limb asymmetry in terms of flare number α_N vanishes (see M list in Table 2), the mean peak flux of limb flares is still more than 18% higher. Their mean duration is also about 5% higher. And their mean integral flux is 13% higher than that of the disc flares.

In temporal sense the effect described above seems to only be observed in odd cycles (for them the asymmetry is even more pronounced: mean limb peak flux is 33% higher, mean integral flux – 31% higher with respect to disc flares, and the mean duration is 8% higher). In even cycles the situation is reversed, with disc flux prevailing (10% higher in mean peak values and 23% higher in mean integral values, however, mean duration is 11% lower for disc flares).

It seems that during the solar maximum the outer and inner flares are mostly uniform in number (4% more disc flares) and demonstrate only small differences in fluxes (in particular, mean limb peak flux is 4% higher, but at the same time in integral flux the disc prevails with 9% difference).

During solar minimum, the centre-to-limb asymmetry is really prominent, with the outer flares constituting 2/3 of all the flares (66% of the total, or 91% higher than the disc flare number; 5.5% probability of this occurring from a uniform distribution). At the same time, their mean fluxes are also noticeably larger (32% difference in peak flux, 16% in the integral flux). The only outlier is a noticeably (32%) smaller mean limb flare duration.

During the rising phase of a cycle the limb flares dominate in number (33% difference), whereas during the falling phase the numbers are equal. Both phases demonstrate higher mean peak flux of limb flares.

An interesting case is the current cycle (number 25), where so far (as of June 2023) limb flare number is 150% higher than the disc flare number (with the mean limb peak flux being 25% higher, and integral flux – 84% higher). This could potentially be attributed to small sample size, yet the p -value is pretty small ($p = 0.09$).

Spearman's coefficient (Table 7) shows weak correlation between the limb proximity during falling phase of a cycle and flares' integral flux ($\rho = 0.127$, $p = 0.134$), peak flux ($\rho = 0.153$, $p = 0.071$), flare duration ($\rho = 0.160$, $p = 0.059$). A stronger correlation is found for peak flux during solar minimum ($\rho = 0.345$, $p = 0.037$).

4.2 North-south asymmetry

With only two exceptions, more flares consistently happen in the southern half of the disc (Table 3) – the difference in number with respect to the northern one ranging from 24% (odd cycles) to 85% (solar minimum). The two exceptions are: cycle 25 (no difference) and the rising phase of a cycle (67% difference in favour of the north). Most of these differences consistently have very low p -values (see Table 5).

Same is true for mean peak and mean integral fluxes that are consistently lower for the flares in the south (difference of mean peak flux ranging from 1% during even cycles to 67% at solar minimum; integral flux – from 13% in even cycles to 92% during solar minimum). The current cycle demonstrates significant dominance of the mean integral flux in the north (105% difference with respect to the south).

The mean flare duration is fluctuating from one list to another, overall being slightly (7%) higher for the southern flares.

A weak anti-correlation (see Table 8) is found between latitude (counting northward) and flare duration during solar maximum and odd cycles ($\rho = -0.105$, $p = 0.144$ and $\rho = -0.117$, $p = 0.105$ correspondingly), as well as the integral flux during the rising phase ($\rho = 0.213$, $p = 0.03$), which confirms the observations outlined above in this section at least for these temporal segments.

4.3 East-west asymmetry

Overall there is a small (4%) prevalence of western flares in numbers (see Table 4), even though it is not consistent over other lists (mostly due to cycle 22 demonstrating 25% prevalence of eastern flares). The p -values are consistently large for all these cases ($p > 0.25$).

In terms of flare durations, mean peak and integral fluxes cycle 22 still demonstrates the highest western dominance

(37%, 38% and 131% difference correspondingly with respect to the eastern flares).

Overall, there is a slight western prevalence in mean flare duration (2%), mean peak flux (8%) and mean integral flux (9%). Much like in the cases of centre-to-limb and north-south asymmetries (see sections 4.1 and 4.2), this general pattern is enhanced during solar minima: they demonstrate 31%, 7% and 28% differences correspondingly.

A weak anti-correlation is found (see Table 8) between longitude (counting westward) and: peak flux in even cycles ($\rho = -0.139$, $p = 0.145$), during solar maximum ($\rho = -0.113$, $p = 0.118$) and cycle 24 ($\rho = -0.217$, $p = 0.063$). A weak correlation is found between longitude and flare duration during solar minimum ($\rho = 0.279$, $p = 0.095$), as well as integral flux during the rising phase of a cycle ($\rho = 0.213$, $p = 0.03$).

4.4 Statistical remarks

Overall there is evidence (Joshi & Chandra 2020) that asymmetries tend to fluctuate over time, following the general evolution of the solar cycles. Hence it seems that a finer temporal resolution is needed, as bigger timeframes (e.g. lists given in Table 1) tend to over-average and erase the finer dynamics of solar activity. However, given the focus on strong flares of this study, it is unreasonable to reduce the time intervals (e.g. to 1 year), as it would greatly reduce the sample size (for some years – down to zero: see section 2.4) and make any results inconclusive. Nevertheless, a 5-year running mean series have been superficially examined (not shown here). Generally the results are consistent with previous studies at least for the north-south asymmetry (Joshi & Joshi 2004). On the other hand, the existence of longer asymmetry cycles have also been suggested (Kraminin & Mikhalina 2019).

Kolmogorov-Smirnov tests (see Table 6) indicate that many of the observed (in section 4) discrepancies do not necessarily represent populational differences, and the differences in mean values of flare durations and fluxes are mostly caused by rare outliers. Calculations of variance (not shown here) of the corresponding flare lists support this hypothesis. The only exception is flare duration, where the variance is typically smaller than the variance in peak and integral flux. This is consistent with studies that show independence of flare strength and duration (Reep & Knizhnik 2019).

5 CONCLUSIONS AND DISCUSSION

The positions and characteristics (duration, peak flux, integral flux) of strong solar flares (X-class) have been examined for the time interval spanning almost 33 years (September 1991 – May 2023) or almost 3 full solar cycles. The three different types of asymmetries (centre-to-limb, north-south, east-west) have been analysed. Detailed results are given in section 4.

The most prominent asymmetry to be found is the north-south asymmetry. It is observed consistently in the full flare list and most of the temporal segments thereof for all three studied parameters. Generally speaking, strong flares have had higher durations, mean peak fluxes and mean integral fluxes in the southern hemisphere over the studied timeframe. The only exceptions are the rising phase of the solar cycle and cycle 22, during both of which the northern hemisphere

has been more active. Both phenomena have been well recognized in the literature: e.g. in Garcia (1990); Joshi et al. (2015). Most likely explanation, it seems, must be related to some intrinsic large-scale asymmetry in the Sun itself, like the long-term differences in the polar magnetic field strength (Svalgaard & Kamide 2012). Notably, the north-south asymmetry is enhanced during the solar minimum.

Regarding the east-west asymmetry, there is a slight prevalence of western flares in terms of the mean flare duration (2%), mean peak flux (8%) and mean integral flux (9%). These differences are mostly caused by rare outliers, which tended to happen more frequently in the west of the solar disc (during the studied time interval). Overall, this result contradicts the findings of Heras et al. (1990). One possible explanation of the discrepancy is their reliance on biased H α observations (see section 2.2). The results of Prasad et al. (2020), on the other hand, support the findings given here. The east-west asymmetry is also enhanced during the solar minimum. Generally, the existence and nature of east-west asymmetry is hard to explain (Li, K.-J. et al. 1998). Perhaps it could be related to the large scale magnetic field arrangements, as has been suspected for gamma ray asymmetries (Harris et al. 2007). A possible hint at this is the existence of east-west asymmetry in the corona as well (Efimov et al. 2002).

Centre-to-limb asymmetry is not present in terms of numbers of flares in the full list. However, the limb flares' mean peak flux is about 18% higher, their mean duration is about 5% higher, and their mean integral flux is 13% higher than that of the disc flares. It is prominent in the rising phase of a cycle and especially during the solar minimum (where 2/3 of all the strong flares happen at the limb – 5.5% probability of this occurring from a uniform distribution). Moreover, during the solar minimum the strong flares exhibit a 32% higher mean peak flux and 16% higher integral flux at the limb. Centre-to-limb variations have been reported for radio waves (Silva & Valente 2002; Kawate et al. 2011), microwaves (Schmahl et al. 1985; Hidalgo Ramírez et al. 2019), EUV (Veselovsky et al. 2001; Thiemann et al. 2018), gamma rays and hard X-rays (Vestrand 1991), however, they are not believed to exist in soft X-rays (McTiernan & Petrosian 1991; Dickson & Kontar 2013). The present study shows that they do exist, and are the most pronounced during the solar minimum.

It seems that, given the uniform flare distribution, the same solar flare would “appear” to be stronger in soft X-rays when it is observed near the limb with respect to a position closer to the central meridian (soon this hypothesis could be directly falsified by stereoscopic X-ray imaging of flare sites by STIX and MiSolFA instruments: Casadei et al. (2017); Xiao et al. (2023)). Possibly, this (as well as the other two asymmetries) is related to large scale magnetic structuring of the Sun, as the asymmetries are enhanced during the solar minimum.

Regardless of the underlying reasons, the proposition is made to call this (the prevalence in number and strength of the strong solar flares at the limb during the solar minimum) Vinny effect¹.

¹ On April 8, 2017 at one of the conferences a gentleman named Vinny has asked the author, “If you discover something, call it Vinny effect.”

ACKNOWLEDGEMENTS

The author would like to thank: Daniel Nigro (aka smAshomAsh²), the discussion with whom has provided the initial inspiration to conduct this research; the Sun, for not being too active after the year 2005, as it has been very time-consuming to process all the previous flares already.

DATA AVAILABILITY

The raw data used in the study are referenced in the text, wherever necessary. The processed data (including the relevant solar images and the final flare list) are freely available at the link: https://drive.google.com/drive/folders/1eUWcwsLAo1HuTm3FRWpvsf5_uC5pm4I3?usp=drive_link.

REFERENCES

- Casadei D., Jeffrey, N. L. S. Kontar, E. P. 2017, *A&A*, 606, A2
 Conway A. J., Matthews S. A., 2003, *A&A*, 401, 1151
 Dickson E. C. M., Kontar E. P., 2013, *Sol. Phys.*, 284, 405
 Efimov A. I., Samoznaev L. N., Andreev V. E., Bird M. K., Edenhofer P., Plettemeier D., Wohlmuth R., 2002, *Advances in Space Res.*, 30, 453
 Garcia H. A., 1990, *Sol. Phys.*, 127, 185
 Harris M. J., Tatischeff V., Kiener J., Gros M., Weidenspointner G., 2007, *A&A*, 461, 723
 Heras A. M., Sanahuja B., Shea M. A., Smart D. F., 1990, *Sol. Phys.*, 126, 371
 Hidalgo Ramirez R. F., Morosi A., Silva D., Simoës P. J. A., Valio A., 2019, *Sol. Phys.*, 294
 Joshi A., Chandra R., 2020, *Open Astron.*, 28, 228
 Joshi B., Joshi A., 2004, *Sol. Phys.*, 219, 343
 Joshi B., Bhattacharyya R., Pandey K. K., Kushwaha U., Moon Y.-J., 2015, *A&A*, 582, A4
 Kawate T., Asai A., Ichimoto K., 2011, *PASJ*, 63, 1251
 Kraminin A. P., Mikhailina F. A., 2019, *Geomagnetism and Aeronomy*, 59, 1096
 Krucker S., et al., 2015, *ApJ*, 802, 19
 Li, K.-J. Schmieder, B. Li, Q.-Sh. 1998, *Astron. Astrophys. Suppl. Ser.*, 131, 99
 Machol J., Codrescu S., Peck C., 2023, User's Guide for GOES-R XRS L2 Products (accessed June 8, 2023), https://data.ngdc.noaa.gov/platforms/solar-space-observing-satellites/goes/goes16/l2/docs/GOES-R_XRS_L2_Data_Users_Guide.pdf
 McTiernan J. M., Petrosian V., 1991, *ApJ*, 379, 381
 Montana State University 2017, Yohkoh Legacy data Archive (accessed June 8, 2023), <https://ylstone.physics.montana.edu/ylegacy/>
 NGDC 2023, Boulder Synoptic Maps (accessed June 8, 2023), <https://www.ngdc.noaa.gov/stp/space-weather/solar-data/solar-imagery/composites/full-sun-drawings/boulder/>
 NOAA 2023, GOES-R Space Weather (accessed June 8, 2023), <https://www.ngdc.noaa.gov/stp/satellite/goes-r.html>
 Pesnell D., 2023, AIA/HMI Browse Data (accessed June 8, 2023), <https://sdo.gsfc.nasa.gov/data/aiahmi/>
 Plutino N., Berrilli F., Del Moro D., Giovannelli L., 2023, *Advances in Space Res.*, 71, 2048
 Prasad A., Roy S., Panja S. C., Patra S. N., 2020, in 2020 IEEE Applied Signal Processing Conference (ASPCON). pp 21–25, doi:10.1109/ASPCON49795.2020.9276656
 Reale F., 2014, *Living Rev. Sol. Phys.*, 11
 Reep J. W., Knizhnik K. J., 2019, *ApJ*, 874, 157
 Roy J.-R., 1977, *Sol. Phys.*, 52, 53
 Schmahl E. J., Kundu M. R., Dennis B. R., 1985, *ApJ*, 299, 1017
 Silva A. V., Valente M. M., 2002, *Sol. Phys.*, 206, 177
 Svalgaard L., Kamide Y., 2012, *ApJ*, 763, 23
 Thiemann E. M. B., Chamberlin P. C., Eparvier F. G., Epp L., 2018, *Sol. Phys.*, 293
 Veselovsky I. S., Zhukov A. N., Dmitriev A. V., Tarsina M. V., Clette F., Cugnon P., Hochedez J. F., 2001, *Sol. Phys.*, 201, 27
 Vestrand W. T., 1991, *Philos. Trans. R. Soc. of London, Series A: Phys. Eng. Sci.*, 336, 349
 Virtual Solar Observatory 2023, (accessed June 8, 2023), <https://sdac.virtualsolar.org/>
 Xiao H., et al., 2023, *A&A*, 673, A142

This paper has been typeset from a $\text{\TeX}/\text{\LaTeX}$ file prepared by the author.

² <https://smashomash.com/>